nature structural & molecular biology

Structural basis for DNA recognition and processing by UvrB

James J Truglio[1,3], Erkan Karakas[1], Benjamin Rhau[1], Hong Wang[2], Matthew J DellaVecchia[2], Bennett Van Houten[2] & Caroline Kisker[1,3]

DNA-damage recognition in the nucleotide excision repair (NER) cascade is a complex process, operating on a wide variety of damages. UvrB is the central component in prokaryotic NER, directly involved in DNA-damage recognition and guiding the DNA through repair synthesis. We report the first structure of a UvrB–double-stranded DNA complex, providing insights into the mechanism by which UvrB binds DNA, leading to formation of the preincision complex. One DNA strand, containing a 3′ overhang, threads behind a β-hairpin motif of UvrB, indicating that this motif inserts between the strands of the double helix, thereby locking down either the damaged or undamaged strand. The nucleotide directly behind the β-hairpin is flipped out and inserted into a small, highly conserved pocket in UvrB.

Nucleotide excision repair (NER) is a conserved DNA-repair system present in all kingdoms of life[1,2]. The system is distinct in its ability to repair a vast array of chemically and structurally distinct DNA lesions[1,3]. The UvrA, UvrB and UvrC proteins mediate NER in prokaryotes in a multistep, ATP-dependent reaction[4,5]. Repair is initiated through the formation of a DNA damage–recognition complex containing either the $UvrA_2$–UvrB heterotrimer[6] or the $UvrA_2$ – $UvrB_2$ heterotetramer[7]. After damage identification, UvrA dissociates, whereas UvrB remains bound to the DNA[8] and forms a stable preincision complex[6,9]. UvrC binds this complex and mediates the sequential incision of the damaged DNA strand 4 nucleotides (nt) toward the 3′ end and 7 nt toward the 5′ end from the lesion[10–12]. Turnover of the UvrBC proteins requires UvrD (helicase II) and DNA polymerase I (pol I)[13,14].

UvrB, the central component in prokaryotic NER, is essential in damage recognition. Several crystal structures of UvrB in the absence of DNA[15–18] have been solved. Of the five domains of UvrB, 1a, 1b, 2, 3 and 4, domain 2 interacts with UvrA and domain 4 interacts with both UvrA and UvrC[19]. UvrB contains six helicase motifs located in domains 1a and 3, making UvrB a member of the helicase superfamily. Domains 1 and 3, which share high structural similarity to the DNA helicases NS3, PcrA and Rep, bind ATP at their domain interface. UvrB contains all of the structural properties of a helicase necessary to couple ATP binding and hydrolysis to domain motion; however, it has only limited strand-separating activity[9,20], and it is likely that domain motions are an essential requirement for damage recognition and formation of the preincision complex.

The most prominent feature of UvrB is a highly conserved and flexible β-hairpin connecting domains 1a and 1b, which is rich in aromatic and hydrophobic residues. The tip of the hairpin interacts with domain 1b through salt bridges and hydrophobic interactions, and the base contains a number of highly conserved aromatic residues. Superposition of UvrB with the structures of monomeric helicase–DNA complexes has suggested that the translocated strand would be partially covered by the β-hairpin, leading to the notion that one of the DNA strands threads behind the β-hairpin[17]. It has also been shown that the DNA can be partially melted over a 3- to 5-base-pair (bp) region in the preincision complex[20–22]. To gain insights into DNA recognition by UvrB, we have determined the crystal structure of this protein from *Bacillus caldotenax* in complex with DNA.

RESULTS

Structure of the UvrB–DNA complex

UvrB was found to bind tightly to a DNA hairpin (hpDNA) with a 3-bp stem, an 11-nucleotide loop and a 3-nt 3′ overhang (**Fig. 1a**). The UvrB–DNA complex contains domains 1a, 1b, 2 and 3 and the β-hairpin motif of UvrB, whereas domain 4 is disordered. Nucleotides C6–C12 of the loop and nucleotide A20 are disordered. The remainder of the hpDNA is well defined, including a partial structure of a fluorescein-adducted thymine (FldT; F11) located in the loop (**Fig. 1a**,**b**). We initially sought to obtain a complex between UvrB and a single-stranded DNA (ssDNA) containing this well-recognized substrate[9,23]. The formation of a DNA hairpin was not anticipated. This fortuitous event revealed the way in which the 3′ overhang

[1]Department of Pharmacological Sciences, Stony Brook University, Stony Brook, New York 11794-5115, USA. [2]Laboratory of Molecular Genetics, National Institute of Environmental Health Sciences, US National Institutes of Health (NIH), Research Triangle Park, North Carolina 27709, USA. [3]Rudolf Virchow Center for Experimental Biomedicine, Institute for Structural Biology, University of Würzburg, Versbacher Str. 9, 97078 Würzburg, Germany. Correspondence should be addressed to C.K. (caroline.kisker@virchow.uni-wuerzburg.de or kisker@pharm.stonybrook.edu).

Received 11 November 2005; accepted 27 January 2006; published online 12 March 2006; doi:10.1038/nsmb1072

threads behind the β-hairpin, forming contacts with domains 1a, 1b and the β-hairpin, whereas the double-stranded DNA (dsDNA) stem is bound by domains 1a and 1b. Electrophoretic mobility shift assays (EMSAs; data not shown) of an identical ssDNA substrate lacking the adduct indicated that it interacts almost as strongly with UvrB. Therefore, the DNA substrate recognized by UvrB is the 3-bp dsDNA with a 3-base 3′ overhang.

The β-hairpin inserts between the DNA strands

The 3′ DNA overhang is clamped behind the β-hairpin of UvrB and forms tight interactions with residues of the β-hairpin and domain 1b (**Figs. 1** and **2**). Overall, the UvrB–DNA structure is similar to the unbound UvrB structure (PDB entry 1T5L) with an r.m.s. deviation of 1.5 Å for 577 of 593 possible Cα atoms. However, the base of the β-hairpin adopts a very different conformation from that of apo UvrB, although the salt bridges and hydrophobic interactions between the tip of the β-hairpin and domain 1b are conserved (**Fig. 1d**). Double-stranded DNA cannot be accommodated behind the β-hairpin without abolishing these interactions. For dsDNA, the second DNA strand must therefore pass in front of the β-hairpin and reanneal with the clamped DNA strand as it emerges from the binding pocket (**Fig. 1a,c**).

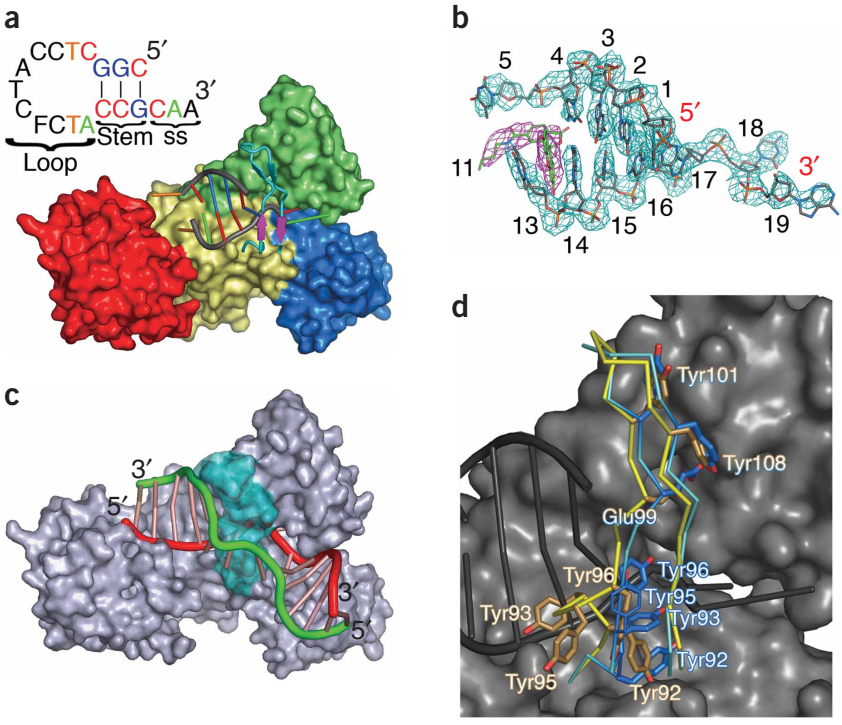

Figure 1 The UvrB–DNA complex and selected electron density. (**a**) Surface of UvrB is color-coded by domain (yellow, 1a; green, 1b; blue, 2; red, 3; cyan, the β-hairpin of UvrB; magenta, the newly formed β-sheet after DNA binding). DNA is illustrated by spokes and letters, color-coded by nucleotide type. The letter representation of the DNA is in a similar orientation to the DNA in the structure. Black letters, disordered nucleotides; F, fluorescein-adducted thymine. The fluorescein-dT, although partially ordered (**Fig. 1b**), has been omitted from the figure for clarity. (**b**) $2F_o - F_c$ electron density map contoured at 1.0 σ covering the DNA. Gray, carbons of unmodified nucleotides; green, carbons of partially ordered fluorescein; magenta, electron density for the fluorescein. Nucleotides are labeled consecutively from 5′ to 3′, omitting numbers of disordered residues. (**c**) UvrB–DNA model showing how the inner strand of the DNA (red) travels between the β-hairpin (cyan) and domain 1b and the outer strand (green) travels around the outside of the β-hairpin. (**d**) Superposition of DNA-bound and apo UvrB. β-hairpin regions of the DNA-bound (cyan and blue) and apo UvrB (PDB entry 1D9X; yellow and gold) are superimposed. Select residues are shown with color-coded labeling. Dark gray spokes represent the bound DNA and the surface of the remainder of the UvrB–DNA complex is shown in gray.

The UvrB-DNA interaction

UvrB interacts predominantly with the DNA strand that is located behind the β-hairpin (A14 to A19; **Fig. 2**), also referred to as the inner strand. Only a few interactions are observed with the outer strand (**Fig. 2** and **Supplementary Table 1** online), suggesting that DNA-stacking interactions rather than protein-DNA interactions hold the outer strand in place. This is reflected in an average *B*-factor of 96.9 $Å^2$ for the outer strand compared to 66.4 $Å^2$ for the inner strand. The surface provided by domain 1a and domain 1b allows a tight approach of the duplex DNA, with a combined buried surface area of 1,575 $Å^2$, maximizing the van der Waals contacts between the protein and the DNA. UvrB forms numerous electrostatic interactions with the inner strand of the duplex region via residues Lys67, Ser91, Ser141, Ser143, Gln346 and Arg357 (**Fig. 2** and **Supplementary Table 1**). Of these residues, only Lys67 is part of a conserved helicase motif (motif Ia in domain 1a). However, the modeled extension of the DNA predicts that it will also interact with motifs IV, V and VI in domain 3 (**Fig. 1c**). Tyr96 and Gln97 interact electrostatically with C1 of the outer strand (**Fig. 2a** and **Supplementary Table 1**).

The outer strand is extended in the 3′ direction beyond the double-stranded region by two additional nucleotides, C4 and T5, the latter of which forms π-stacking interactions with Phe527, thereby approaching domain 3 (**Fig. 2a**). Phe527 is highly conserved and may be important for positioning the DNA for the incision reaction, as shown by reduced incision efficiency when this residue is mutated to alanine[23]. Further supporting its role, our structure shows that the helical axis of the DNA is aligned in such a way that the DNA will be in close proximity to this residue. Understanding of the precise role of Phe527 has to await a structure with a longer DNA duplex. The inner strand is also extended by two nucleotides, T13 and A14, beyond the double-stranded region toward the 5′ end (**Fig. 2a**). These extensions form a hydrophobic pocket, which provides a binding site for the fluorescein adduct (**Fig. 1b**).

The C1-G17 base pair adjacent to the 3′ overhang stacks against the strictly conserved residues Pro98 and Tyr96 of the β-hairpin (**Fig. 2**). Mutation of Tyr96 to alanine results in loss of UvrC incision, lack of formation of the UvrB–DNA preincision complex and less than 6% of wild-type UvrB's strand-destabilization activity[23]. In the UvrB–DNA complex, Tyr96 forms π-stacking interactions with G17, occupying the position of C18 that is unavailable for stacking interactions with neighboring bases, as it is flipped out of the double helix behind the β-hairpin. Thus, Tyr96 is crucial in stabilizing the separated DNA strands[23].

Base flipping

C18 is located behind the β-hairpin in a narrow, hydrophobic pocket, which only provides space for a planar molecule. The base fits tightly into this pocket and forms π-stacking interactions with Phe249 (**Fig. 2c**),

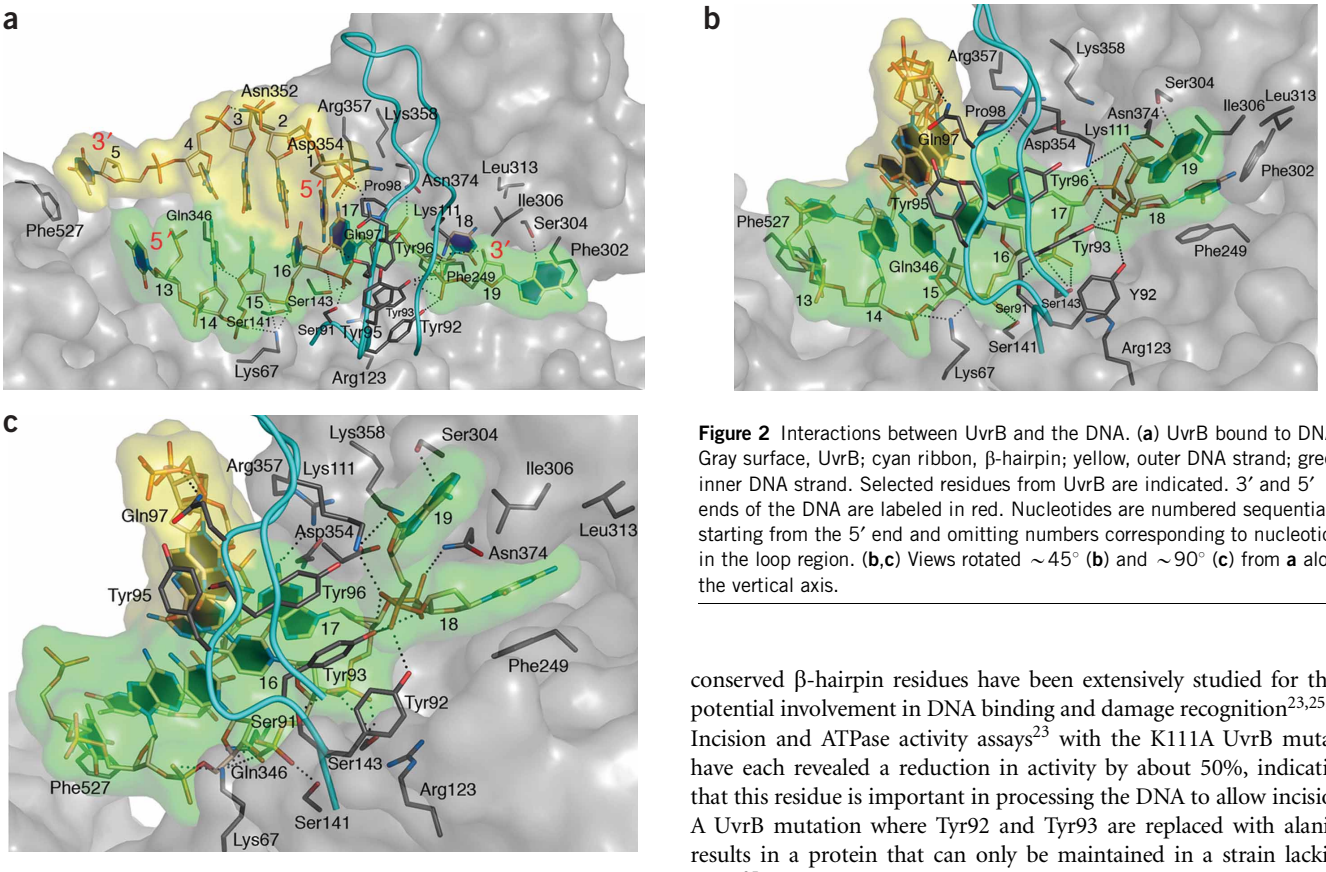

Figure 2 Interactions between UvrB and the DNA. (**a**) UvrB bound to DNA. Gray surface, UvrB; cyan ribbon, β-hairpin; yellow, outer DNA strand; green, inner DNA strand. Selected residues from UvrB are indicated. 3′ and 5′ ends of the DNA are labeled in red. Nucleotides are numbered sequentially starting from the 5′ end and omitting numbers corresponding to nucleotides in the loop region. (**b**,**c**) Views rotated ~45° (**b**) and ~90° (**c**) from **a** along the vertical axis.

a highly conserved residue that is substituted by histidine or tyrosine only in certain species. Notably, mutation of Phe249 to alanine has little effect on the activity of UvrB *in vitro* other than a modest reduction (~22%) in ATPase activity[23]. In fact, cross-linking experiments suggest that the alanine replacement facilitates the formation of the UvrB–DNA complex[24]. Widening of the pocket by mutating Phe249 may ease binding of an extruded nucleotide into this altered region. The type-conserved residues Ile306 and Leu313 complete the remainder of the pocket (**Fig. 2**), which is deep enough to accommodate both purine and pyrimidine bases. The sides of the pocket are open to the solvent, allowing nucleotides to enter and exit. To enter the pocket, C18 has to rotate behind the β-hairpin, where it passes a patch of highly conserved, charged residues: Asp354, Arg357 and Lys358 (**Fig. 2**). The structure suggests that these residues provide a path for unmodified bases to enter the binding pocket.

Exiting the pocket

The next nucleotide, A19, initiates the transition where the DNA emerges from behind the β-hairpin. The base of A19 extends out from behind the β-hairpin and into the solvent, forming van der Waals contacts with Phe302 and a hydrogen bond to the side chain of Ser304, neither of which is conserved (**Figs. 1** and **2**). The phosphate and ribose atoms of this nucleotide, by contrast, are buried and tightly bound between the base of the β-hairpin and domain 1b (**Fig. 2**). The phosphate oxygen atoms form hydrogen bonds with the hydroxyl groups of Tyr92 and Tyr93 as well as the ε-amino group of Lys111, a residue that also interacts with the ribose of A19. Tyr93 also forms a hydrogen bond to the 3′-OH group of C18 (**Fig. 2**). All of these highly conserved β-hairpin residues have been extensively studied for their potential involvement in DNA binding and damage recognition[23,25,26]. Incision and ATPase activity assays[23] with the K111A UvrB mutant have each revealed a reduction in activity by about 50%, indicating that this residue is important in processing the DNA to allow incision. A UvrB mutation where Tyr92 and Tyr93 are replaced with alanine results in a protein that can only be maintained in a strain lacking UvrA[25], as the presence of UvrA leads to a lethal phenotype owing to strong binding of UvrB to undamaged DNA. *In vitro* incision assays using the double mutant have shown that undamaged DNA is efficiently incised. However, the mutant is not deficient in recognizing damaged DNA, and it has been suggested that these two residues are not necessarily involved in damage recognition, but that rather they prevent binding of UvrB to undamaged DNA. *In vivo* experiments with the individual tyrosine-to-alanine substitutions have revealed that these mutations can only be maintained in strains lacking UvrA or the endonucleases UvrC and Cho, which suggests that both damaged and undamaged DNA is incised[26]. *In vitro* experiments have shown that the Y93A mutant is considerably more affected than the Y92A mutant in all assays[23]. The structure of the UvrB–DNA complex shows that Tyr92, Tyr93 and Tyr96 form an aromatic chain stabilized by π-stacking interactions. As Tyr93 is located in the middle of this chain, its mutation to alanine affects not only Tyr92, but most probably also Tyr96, strongly supporting the *in vitro* data in which a more severe phenotype of the Y93A mutant has been observed[23].

UvrB moves in a 3′→5′ direction

With the 3-nt 3′ overhang inserted behind the β-hairpin, the structure reveals that UvrB is able to translocate along ssDNA in a 3′→5′ direction. However, *in vivo*, the combined action of UvrA, UvrB and ATP is required to achieve strand separation in the context of dsDNA. It is generally assumed that UvrA facilitates strand opening and thereby allows the insertion of UvrB's β-hairpin in between the two DNA strands. ATP hydrolysis by UvrB is necessary for further strand separation and damage verification. NS3 helicase, UvrB's closest structural homolog, is a 3′→5′-acting helicase, as are structurally related helicases Rep and PcrA. In keeping with this relationship, the

orientation of the strand passing under the β-hairpin has the same polarity as for NS3 (ref. 17).

The outer DNA strand

According to our structure and biochemical data[27], Tyr95 is solvent exposed and is predicted to interact with the outer DNA strand as it passes over the β-hairpin (**Fig. 2**). Furthermore, it has been shown that, independent of UvrA, the Y95W variant binds tightly (K_d = 88.4 ± 3.7 nM) to DNA with a lesion located in an unpaired bubble region and less tightly to a similar, undamaged bubble-DNA substrate, suggesting that Tyr95 may interact with the adduct. We generated the Y95A variant, which shows a 30% reduction in binding affinity for a 50-mer dsDNA with a central fluorescein adduct and a 35% decrease in incision when used in a complete UvrABC-reconstituted system (**Supplementary Fig. 1** online).

In combination with our structure, these results imply that the damaged strand is the outer strand and the damage is in close proximity to Tyr95. Several experiments support this conclusion. Photolyase has been observed to bind and act on a pyrimidine dimer in a preformed UvrA–UvrB–DNA preincision complex. In addition, UvrABC, unlike T4 endonuclease V, can incise a pyrimidine dimer bound by photolyase[28]. The structure of the photolyase–pyrimidine dimer complex has revealed that the pyrimidine dimer flips out of the DNA and into an active site cavity in the protein[29]. To gain access to the pyrimidine dimer in the UvrB–DNA preincision complex, the damage would have to be located on the surface of UvrB, which would further suggest that it is located on the outer strand, where it would be more accessible.

The inner DNA strand

While this manuscript was under review, Malta *et al.* reported on a study using the fluorescent properties of 2-aminopurine (2-AP) to investigate nucleotide flipping in the UvrB–DNA complex[30]. 2-AP was placed at various positions around a cholesterol-DNA adduct. These data clearly show that the base adjacent to the lesion on the 3′ side is extrahelical in the UvrB–DNA complex. Furthermore, lack of fluorescence quenching and a blue shift in fluorescence, indicative of an environment with a lower dielectric constant, suggest that the base is flipped into a pocket in UvrB. According to our structure, these data could describe the flipped nucleotide behind the β-hairpin, which would be relatively inaccessible and located in a hydrophobic, low-dielectricity environment. Thus, the damaged nucleotide would be in the position of G17 on the inner strand, stacking with Tyr96 (**Fig. 2**).

DISCUSSION

The use of special DNA damage–containing substrates alleviates the requirement for the presence of UvrA, revealing that UvrB is sufficient for damage recognition[31,32]. It is generally assumed that UvrA initially recognizes DNA perturbations and loads UvrB in close proximity to the putative lesion, and UvrB then analyzes the perturbation to verify the lesion. Our structure reveals that UvrB interacts with DNA by inserting its β-hairpin between the strands of the duplex DNA, locking one of the strands between the β-hairpin and domain 1b. As UvrB cannot bind regular damaged dsDNA, UvrA's role may be to melt the DNA and promote separation of UvrB's β-hairpin from domain 1b, allowing its insertion between the DNA strands. Upon DNA binding, the ATPase activity of UvrB is activated, leading to a 3′→5′ translocation, according to our structure. UvrB has limited helicase activity and can translocate only a few nucleotides along the clamped strand in search of the lesion. During translocation, each consecutive nucleotide of this strand is flipped behind the β-hairpin into a hydrophobic nucleotide-binding pocket. Tyr96 stabilizes the opening of the dsDNA by substituting for the extruded base.

DNA in the preincision complex is dramatically bent[33]. This distortion is crucial for incision by UvrC, as no incision is observed when using the *Escherichia coli* UvrB D478A variant, which can bind but not bend DNA[34]. The nucleotide-binding pocket created by residues Phe249, Ile306 and Leu313 may provide a 'grip' for UvrB on the DNA, aiding in DNA distortion and stabilizing the preincision complex.

Although this UvrB–DNA structure has provided great insight into the DNA-binding mode of UvrB, it is still not clear whether the damage is located on the inner or outer strand. Several studies suggest it is located on the outer strand and interacts directly with Tyr95, which is solvent exposed on the outside of the β-hairpin in the structure[27,28]. However, other experiments indicate that the damage is located on the inner strand at the position of G17 (ref. 30). In light of our structure, the latter suggestion is more easily explained. If the damage were positioned at G17, it would be the next base to be translocated behind the β-hairpin into a shape-complementary (planar) pocket after passing a patch of highly conserved, charged residues. Thus, damage recognition of structurally unrelated adducts may be achieved by allowing only undamaged nucleotides to rotate. Damaged nucleotides would be occluded owing to steric hindrance, arresting translocation. Subsequent ATP hydrolysis by UvrB, which is required upon damage recognition before the first incision[35], would distort the DNA rather than translocate it, forming the preincision complex and priming the DNA for cleavage by UvrC. Notably, individual substitutions of alanine for residues Tyr92 and Tyr93, which interact with the flipped nucleotide and the nucleotide exiting from behind the β-hairpin, result in incision of undamaged DNA *in vivo*[25]. These mutations may interfere with translocation similarly to a lesion and lead UvrB to 'falsely assume' that damage has been encountered.

METHODS

Protein expression, purification and crystallization. Expression and purification of *B. caldotenax* UvrB has been described previously[9,23]. To obtain the protein–DNA complex, a solution containing 16 mg ml^{-1} UvrB in 500 mM NaCl and 20 mM Tris-HCl (pH 8.0) was mixed with the DNA substrate, 5′-CGGCTCCATC-FldT-CTACCGCAA-3′ (Sigma-Genosys), in a 1:1.2 molar ratio, and incubated for 1 h. The mixture was dialyzed against a solution containing 150 mM NaCl and 20 mM Tris-HCl (pH 8.0) for 4 h. Crystals of the UvrB–DNA complex were grown using vapor diffusion by mixing equal volumes of the dialyzed sample and precipitant solution (20 mM $MgCl_2$, 14% (w/v) PEG 3000, 80 mM sodium citrate (pH 5.5)) and equilibrating this mixture against a reservoir solution containing 18% (w/v) PEG 3000 and 0.1 M sodium citrate (pH 5.5). Crystals were first transferred through precipitant solutions containing increasing amounts of glycerol in increments of 5% (v/v) until a final concentration of 30% (v/v) was reached and then cryo-cooled in liquid nitrogen.

Structure determination. Data were collected on beamline X26C of the National Synchrotron Light Source at Brookhaven National Laboratory, equipped with an ADSC Quantum 4R detector. Diffraction data (**Table 1**) were indexed and scaled using the HKL2000 software[36]. Crystals contained two UvrB–DNA complexes per asymmetric unit. The structure was solved by molecular replacement using AmoRe[37] with the structure of the Y96A variant of UvrB from *B. caldotenax* (PDB entry 1T5L) as a search model. The resulting model was rebuilt and the DNA added using O[38] and the structure was refined using REFMAC[37]. Additional calculations were performed using the CCP4 suite[37]. The final model has 86.2% of its residues in the most favored regions of the Ramachandran plot and 0.5% in disallowed regions, as defined by PROCHECK[39].

Table 1 Data collection and refinement statistics

	UvrB–DNA complex
Data collection	
Space group	$P3_221$
Cell dimensions	
a, *b*, *c* (Å)	153.4, 153.4, 160.7
Resolution (Å)	50–3.3 (3.4–3.3)
R_{sym}	13.8 (54.8)
$I/\sigma I$	19.4 (5.0)
Completeness (%)	99.9 (100.0)
Redundancy	7.8 (7.9)
Refinement	
Resolution (Å)	3.3
No. reflections	33,177
R_{work} / R_{free}	20.5 / 25.8
No. atoms	
Protein	8,803
Ligand/ion	375 (DNA)
B-factors	
Protein	74.2
Ligand/ion	78.6 (DNA)
R.m.s. deviations	
Bond lengths (Å)	0.016
Bond angles (°)	1.3

Numbers in parentheses refer to the highest-resolution data shell.

Accession codes. Protein Data Bank: Coordinates have been deposited with accession code 2FDC.

Note: Supplementary information is available on the Nature Structural & Molecular Biology website.

ACKNOWLEDGMENTS

This work has been supported by grants to C.K. from the NIH (GM 070873) and from the Pew Scholars Program in the Biomedical Sciences, and in part by the Intramural Research Program of the National Institute of Environmental Health Sciences, NIH (B.V.H.). The National Synchrotron Light Source in Brookhaven is supported by the US Department of Energy and the NIH, and beamline X26C is supported in part by the State University of New York at Stony Brook and its Research Foundation.

COMPETING INTERESTS STATEMENT

The authors declare that they have no competing financial interests.

Published online at http://www.nature.com/nsmb/
Reprints and permissions information is available online at http://npg.nature.com/reprintsandpermissions/

1. Friedberg, E.C., Walker, G.C. & Siede, W. DNA repair and mutagenesis. (ASM Press, Washington, D.C., 1995).
2. Sancar, A. DNA excision repair. *Annu. Rev. Biochem.* **65**, 43–81 (1996).
3. Lloyd, R.S. & Van Houten, B. DNA damage recognition. in *DNA Repair Mechanisms: Impact on Human Diseases and Cancer* (ed. Vos, J.-M.) 25–66 (R.G. Landes Company, Biomedical Publishers, Austin, Texas, 1995).
4. Goosen, N. & Moolenaar, G.F. Role of ATP hydrolysis by UvrA and UvrB during nucleotide excision repair. *Res. Microbiol.* **152**, 401–409 (2001).
5. Van Houten, B. Nucleotide excision repair in *Escherichia coli*. *Microbiol. Rev.* **54**, 18–51 (1990).
6. Theis, K. *et al.* The nucleotide excision repair protein UvrB, a helicase-like enzyme with a catch. *Mutat. Res.* **460**, 277–300 (2000).
7. Verhoeven, E.E., Wyman, C., Moolenaar, G.F. & Goosen, N. The presence of two UvrB subunits in the UvrAB complex ensures damage detection in both DNA strands. *EMBO J.* **21**, 4196–4205 (2002).
8. Orren, D.K. & Sancar, A. Formation and enzymatic properties of the UvrB-DNA complex. *J. Biol. Chem.* **265**, 15796–15803 (1990).
9. Skorvaga, M., Theis, K., Mandavilli, B.S., Kisker, C. & Van Houten, B. The beta-hairpin motif of UvrB is essential for DNA binding, damage processing, and UvrC-mediated incisions. *J. Biol. Chem.* **277**, 1553–1559 (2002).
10. Lin, J.-J. & Sancar, A. Active site of (A)BC excinuclease: I. Evidence for 5′ incision by UvrC through a catalytic site involving Asp^{399}, Asp^{438}, and His^{538} residues. *J. Biol. Chem.* **267**, 17688–17692 (1992).
11. Sancar, A. & Rupp, W.D. A novel repair enzyme: UvrABC excision nuclease of *Escherichia coli* cuts a DNA strand on both sides of the damaged region. *Cell* **33**, 249–260 (1983).
12. Verhoeven, E.E., van Kesteren, M., Moolenaar, G.F., Visse, R. & Goosen, N. Catalytic sites for 3′ and 5′ incision of *Escherichia coli* nucleotide excision repair are both located in UvrC. *J. Biol. Chem.* **275**, 5120–5123 (2000).
13. Caron, P.R., Kushner, S.R. & Grossman, L. Involvement of helicase-II (UvrD gene product) and DNA Polymerase-I in excision mediated by the UvrABC protein complex. *Proc. Natl. Acad. Sci. USA* **82**, 4925–4929 (1985).
14. Husain, I., Houten, B.V., Thomas, D.C., Abdel-Monem, M. & Sancar, A. Effect of DNA polymerase I and DNA helicase II on the turnover rate of UvrABC excision nuclease. *Proc. Natl. Acad. Sci. USA* **82**, 6774–6778 (1985).
15. Machius, M., Henry, L., Palnitkar, M. & Deisenhofer, J. Crystal structure of the DNA nucleotide excision repair enzyme UvrB from *Thermus thermophilus*. *Proc. Natl. Acad. Sci. USA* **96**, 11717–11722 (1999).
16. Nakagawa, N. *et al.* Crystal structure of *Thermus thermophilus* HB8 UvrB protein, a key enzyme of nucleotide excision repair. *J. Biochem.* **126**, 986–990 (1999).
17. Theis, K., Chen, P.J., Skorvaga, M., Houten, B.V. & Kisker, C. Crystal structure of UvrB, a DNA helicase adapted for nucleotide excision repair. *EMBO J.* **18**, 6899–6907 (1999).
18. Truglio, J.J. *et al.* Interactions between UvrA and UvrB: the role of UvrB's domain 2 in nucleotide excision repair. *EMBO J.* **23**, 2498–2509 (2004).
19. Hsu, D.S., Kim, S.T., Sun, Q. & Sancar, A. Structure and function of the UvrB protein. *J. Biol. Chem.* **270**, 8319–8327 (1995).
20. Gordienko, I. & Rupp, W.D. The limited strand-separating activity of the UvrAB protein complex and its role in the recognition of DNA damage. *EMBO J.* **16**, 889–895 (1997).
21. Visse, R., King, A., Moolenaar, G.F., Goosen, N. & van de Putte, P. Protein-DNA interactions and alterations in the DNA structure upon UvrB-DNA preincision complex formation during nucleotide excision repair in *Escherichia coli*. *Biochemistry* **33**, 9881–9888 (1994).
22. Zou, Y. & Van Houten, B. Strand opening by the $UvrA_2B$ complex allows dynamic recognition of DNA damage. *EMBO J.* **18**, 4889–4901 (1999).
23. Skorvaga, M. *et al.* Identification of residues within UvrB that are important for efficient DNA binding and damage processing. *J. Biol. Chem.* **279**, 51574–51580 (2004).
24. DellaVecchia, M.J. *et al.* Analyzing the handoff of DNA from UvrA to UvrB utilizing DNA-protein photoaffinity labeling. *J. Biol. Chem.* **279**, 45245–45256 (2004).
25. Moolenaar, G.F., Hoglund, L. & Goosen, N. Clue to damage recognition by UvrB: residues in the beta-hairpin structure prevent binding to non-damaged DNA. *EMBO J.* **20**, 6140–6149 (2001).
26. Moolenaar, G.F., Schut, M. & Goosen, N. Binding of the UvrB dimer to non-damaged and damaged DNA: residues Y92 and Y93 influence the stability of both subunits. *DNA Repair (Amst.)* **4**, 699–713 (2005).
27. Zou, Y. *et al.* DNA damage recognition of mutated forms of UvrB proteins in nucleotide excision repair. *Biochemistry* **43**, 4196–4205 (2004).
28. Sancar, A., Franklin, K.A. & Sancar, G.B. *Escherichia coli* DNA photolyase stimulates uvrABC excision nuclease in vitro. *Proc. Natl. Acad. Sci. USA* **81**, 7397–7401 (1984).
29. Mees, A. *et al.* Crystal structure of a photolyase bound to a CPD-like DNA lesion after in situ repair. *Science* **306**, 1789–1793 (2004).
30. Malta, E., Moolenaar, G.F. & Goosen, N. Base flipping in nucleotide excision repair. *J. Biol. Chem.* **281**, 2184–2194 (2006).
31. Zou, Y., Walker, R., Bassett, H., Geacintov, N.E. & Houten, B.V. Formation of DNA repair intermediates and incision by the ATP-dependent UvrB-UvrC endonuclease. *J. Biol. Chem.* **272**, 4820–4827 (1997).
32. Moolenaar, G.F. *et al.* The effect of the DNA flanking the lesion on formation of the UvrB-DNA preincision complex. *J. Biol. Chem.* **275**, 8038–8043 (2000).
33. Shi, Q., Thresher, R., Sancar, A. & Griffith, J. Electron microscopic study of (A)BC excinuclease—DNA is sharply bent in the UvrB-DNA complex. *J. Mol. Biol.* **226**, 425–432 (1992).
34. Lin, J.J., Phillips, A.M., Hearst, J.E. & Sancar, A. Active site of (A)BC excinuclease: II. Binding, bending and catalysis mutants of UvrB reveal a direct role in 3′ and an indirect role in 5′ incision. *J. Biol. Chem.* **267**, 17693–17700 (1992).
35. Verhoeven, E.E., Wyman, C., Moolenaar, G.F., Hoeijmakers, J.H. & Goosen, N. Architecture of nucleotide excision repair complexes: DNA is wrapped by UvrB before and after damage recognition. *EMBO J.* **20**, 601–611 (2001).
36. Otwinowski, Z. & Minor, W. Processing of X-ray diffraction data collected in oscillation mode. *Methods Enzymol.* **276**, 307–326 (1997).
37. Collaborative Computational Project, Number 4. The CCP4 suite: programs for protein crystallography. *Acta Crystallogr. D Biol. Crystallogr.* **50**, 760–763 (1994).
38. Jones, T.A., Zou, J.Y., Cowan, S.W. & Kjeldgaard, M. Improved methods for building protein models in electron density maps and the location of errors in these models. *Acta Crystallogr. A* **47**, 110–119 (1991).
39. Laskowski, R.A., McArthur, M.W., Moss, D.S. & Thornton, J.M. PROCHECK—a program to check the stereochemical quality of protein structures. *J. Appl. Crystallogr.* **26**, 283–291 (1993).